Biophysical Chemistry 244 (2019) 1–10

Contents lists available at ScienceDirect

Biophysical Chemistry

journal homepage: www.elsevier.com/locate/biophyschem

Mixing behaviour of bilayer-forming phosphatidylcholines with single-chain alkyl-branched bolalipids: effect of lateral chain length

Sindy Müller[a], Maximilian Kind[a], Kai Gruhle[a], Gerd Hause[b], Annette Meister[c], Simon Drescher[a,*]

[a] Institute of Pharmacy, Biophysical Pharmacy, Martin Luther University (MLU) Halle-Wittenberg, Wolfgang-Langenbeck-Str. 4, Halle (Saale) 06120, Germany
[b] Biocenter, MLU Halle-Wittenberg, Weinbergweg 22, Halle (Saale) 06120, Germany
[c] HALOmem and Institute of Biochemistry and Biotechnology, MLU Halle-Wittenberg, Kurt-Mothes-Str. 3a, Halle (Saale) 06120, Germany

HIGHLIGHTS

- Single-chain alkyl-branched bolalipids show different miscibility with phospholipids
- In mixtures with DPPC, a phase separation is observed
- In mixtures with POPC/DOPC, a miscibility is observed
- Degree of miscibility can be tuned by the length of bolalipid' lateral alkyl chain
- Stable bolasomes are formed by bolalipid:POPC/DOPC 1:4 mixtures

GRAPHICAL ABSTRACT

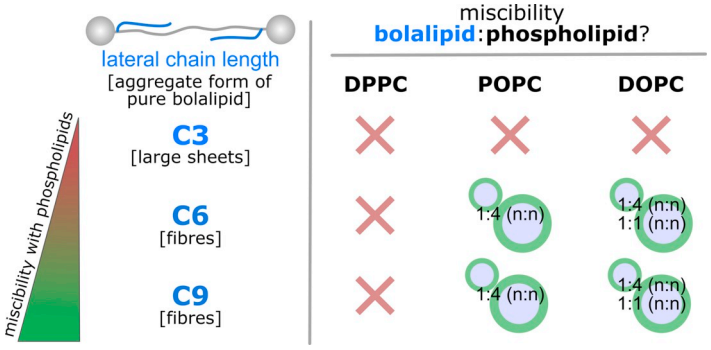

ARTICLE INFO

Keywords:
Bolalipids
Bolaamphiphiles
Phospholipids
Mixing behaviour
Liposomes
Bolasomes

ABSTRACT

Liposomes are a promising class of drug delivery vehicles. However, no liposomal formulation has been approved for an oral application so far, due to stability issues of the liposomes in the gastrointestinal tract. Herein, we investigate the miscibility of three novel single-chain alkyl-branched bolalipids **PC-C32(1,32C*n*)-PC** (n = 3, 6, 9) with either saturated or unsaturated phosphatidylcholines by means of differential scanning calorimetry (DSC), transmission electron microscopy (TEM) of stained samples, vitrified specimens, or replica of freeze-fractured samples, and dynamic light scattering (DLS). The novel bolalipids contain lateral alkyl chains of different length in 1- and 32-position of the long membrane-spanning C32 alkyl chain. We will show for the first time that these single-chain alkyl-branched bolalipids show a miscibility with bilayer-forming phospholipids—by maintaining the vesicular aggregate structure—due to the lateral alkyl substituents located next to the phosphocholine headgroup of the bolalipid. We are convinced that these alkyl side chains are able to fill the void volume, which is created when unmodified single-chain bolalipids are inserted in a transmembrane fashion into a phospholipid bilayer. Consequently, the miscibility of our alkyl-chained bolalipids with bilayer-forming phospholipids rose with increasing lengths of the lateral alkyl chain of the bolalipid. Finally, we were successful in preparing liposomes from various bolalipid/phospholipid mixtures, which were stable in size upon storage for at least 21 days. These mixed liposomes (bolasomes) could be used as oral drug delivery systems in the near future.

* Corresponding author.
E-mail address: simon.drescher@pharmazie.uni-halle.de (S. Drescher).

https://doi.org/10.1016/j.bpc.2018.10.003
Received 4 September 2018; Received in revised form 8 October 2018; Accepted 16 October 2018
Available online 24 October 2018

1. Introduction

Bolaamphiphiles or bolalipids [1] are molecules consisting of one or two long hydrophobic alkyl chains with two polar headgroups attached to each end of the alkyl spacer. This special kind of lipid can be found in the cell membranes of certain species of archaea, *e.g. thermoacidophiles* [2], where they are responsible for the outstanding stability of archaea against harsh living conditions, such as low pH-values, high temperatures, and/or high salt concentrations [3–7]. Since bolalipids are able to span a phospholipid bilayer membrane [8–11], it is reasonable to use this kind of lipid for the stabilization of liposomal formulations composed of conventional, bilayer-forming phosphatidylcholines against the conditions found in the gastrointestinal tract (GIT), *i.e.* the presence of lipases, gastric acids, or bile salts.

The extraction of archaea using organic solvents is a common method to obtain sufficient amounts of the bolalipid material. However, this process is expensive and time-consuming due to the elaborate cultivation conditions of the archaea and the low yield of bolalipid material [12]. Moreover, the extraction procedure always results in a mixture of various bolalipids with different alkyl chain pattern. On the other hand, the total synthesis of the naturally occurring bolalipids, published firstly by Kakinuma and co-workers [13–15], is also very time-consuming and hence not suitable for the production of bolalipid material in larger scale. Thus, it is necessary and promising to simplify the chemical structure of the natural bolalipids while maintaining their stabilizing properties. We and other groups have taken this approach in recent years [16–21].

We have shown earlier that the **PC-C32-PC** (Fig. 1), which represents a very simple archaeal model lipid composed of one single and unmodified C32 alkyl chain and two phosphocholine (PC) headgroups [22,23], shows no tendency to be incorporated into bilayers of different saturated and unsaturated phosphatidylcholines [24,25]. The reason therefore can be found in packing problems that occur when **PC-C32-PC** is mixed with phospholipids: due to the larger space requirement of the PC headgroup of the bolalipid compared to the small cross-sectional area of its single and unmodified alkyl chain, void volume is created when the bolalipid is inserted in a membrane-spanning fashion into the phospholipid bilayer (see schematic representation in Fig. 1, top). As a consequence, both lipid components show a separation and the bolalipid self-assembles into helical nanofibres, whereas the phospholipid forms vesicles [24]. Increasing the cross-sectional area of the hydrophobic part of the bolalipid could circumvent this packing problem and could lead to mixed bolalipid/phospholipid vesicles (bolasomes). On the one hand, one could 'go back' from singles-chain to double-chain bolalipids [26–28]. But, especially the synthesis of diglycerol tetraether lipids is very time-consuming and we discarded this strategy for the moment. On the other hand, one could insert different heteroatoms [17,29], acetylene [25,30] or diacetylene groups [31], methyl branches [25,30], and phenyl [32–36] or biphenyl substituents [33], respectively, into the single alkyl chain of the bolalipid. Using these alkyl-modified bolalipids in mixing studies with bilayer-forming phospholipids, we indeed observe an increased miscibility between both lipid components [25,35,36]. However, closed vesicular aggregates (liposomes) are not formed in the mixed bolalipid/phospholipid systems and wormlike micelles as well as small bilayer fragments (nanodiscs) are found instead [36]. It is plausible that the structural changes of the single-chain bolalipids, *i.e.* the insertion of various perturbations within the alkyl chain, are not sufficient to circumvent the packing problems that occur in bolalipid/phospholipid mixtures. Consequently, the formation of stabilized liposomes using modified single-chain bolalipids in mixture with bilayer-forming phospholipids has not been noticed so far.

To further increase the space requirement of the bolalipid' alkyl chain, we have recently synthesized a set of single-chain bolalipids bearing alkyl substituents of different length in 1- and 32-position of the membrane-spanning C32 chain (Fig. 1, bottom) [37]. These single-chain alkyl-branched bolalipids self-assemble into either lamellar sheets (C3 side chain) or nanofibres (C6 and C9) depending on the length of the lateral alkyl chain.

In this study, we investigated the miscibility of these single-chain alkyl-branched bolalipids **PC-C32(1,32C*n*)-PC** (n = 3, 6, 9) with different bilayer-forming phospholipids, namely 1,2-dipalmitoyl-*sn*-glycero-3-phosphocholine (DPPC), 1-palmitoyl-2-oleoyl-*sn*-glycero-3-phosphocholine (POPC), or 1,2-dioleoyl-*sn*-glycero-3-phosphocholine (DOPC). Investigations were carried out by means of differential scanning calorimetry (DSC) and transmission electron microscopy (TEM) of negatively stained samples, vitrified specimens (cryo-TEM), and replica of freeze-fractured samples (FFEM), respectively. The liposomes from different bolalipid/phospholipid mixtures were prepared by the extrusion method and they were further characterized by means of dynamic light scattering (DLS) right after the preparation and also after different times of storage.

2. Experimental section

2.1. Chemicals

1,2-Dipalmitoyl-*sn*-glycero-3-phosphocholine (DPPC), 1-palmitoyl-2-oleoyl-*sn*-glycero-3-phosphocholine (POPC), and 1,2-dioleoyl-*sn*-glycero-3-phosphocholine (DOPC) were purchased from Avanti Polar Lipids (Alabaster, USA) and used without further purification. Buffer salts were obtained from Sigma Aldrich Co. (Steinheim, Germany). The synthesis of the bolalipid compounds PC-C32(1,32C*n*)-PC (n = 3, 6, 9)

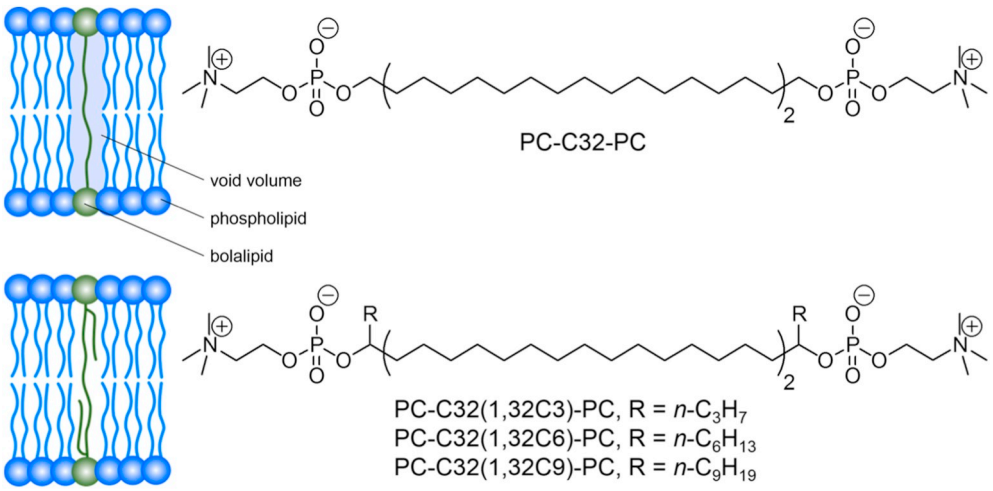

Fig. 1. Left: Schematic representation of a phospholipid bilayer containing a bilayer-forming phospholipid (blue) and either the bolalipid **PC-C32-PC** (top, green) or one of the novel alkyl-substituted bolalipids **PC-C32(1,32C*n*)-PC** (bottom, green) in a membrane-spanning conformation. Right: Chemical structure of **PC-C32-PC** (top) and **PC-C32(1,32C*n*)-PC** (bottom). (For interpretation of the references to colour in this figure legend, the reader is referred to the web version of this article.)

was described previously [37].

2.2. Methods

2.2.1. Sample preparation

Samples of pure lipids were prepared by suspending the appropriate amount of bolalipid or phospholipid in aqueous PBS (pH = 7.4). Homogeneous suspensions were obtained by heating to 70 °C and vortexing. Binary lipid mixtures were prepared from lipid stock solutions in $CHCl_3$/MeOH (2/1, *v*/v) as solvent by mixing appropriate volumes of the stock solutions. The organic solvent was then removed in a stream of nitrogen. The resulting lipid films were kept in an evacuated flask for 24 h to remove residual traces of solvent. The suspensions were then prepared by adding a certain volume of aqueous PBS (pH = 7.4) to obtain a total lipid concentration of 3 mM. The samples were vigorously vortexed for 5 min at 70 °C to obtain a homogenous suspension. Liposomes were prepared by extrusion (31 times) of the lipid suspension through a polycarbonate membrane (100 nm) at a temperature approximately 10 K above the transition temperature observed in the DSC experiments. Aqueous suspensions of lipid mixtures containing POPC and DOPC were stored at 4 °C in a glass vial filled with nitrogen to prevent oxidation.

2.2.2. Differential scanning calorimetry (DSC)

DSC measurements were performed using a MicroCal VP-DSC differential scanning calorimeter (MicroCal Inc. Northampton, MA, USA). Before the measurements, the sample suspension and the reference were degassed under vacuum while stirring. A heating rate of 60 K h^{-1} was used, and the measurements were performed in the temperature interval from 5 °C to 90 °C. To check the reproducibility, three consecutive scans were recorded for each sample. The buffer/buffer baseline was subtracted from the thermogram of the sample, and the DSC scans were evaluated using MicroCal Origin 8.0 software.

2.2.3. Transmission electron microscopy (TEM)

The stained samples were prepared by spreading 5 μL of the lipid suspension (c = 120 μM) onto a copper grid coated with a Formvar film. After 1 min, excess liquid was blotted off with filter paper and 5 μL of 1% aqueous uranyl acetate solution were placed onto the grid and drained off after 1 min, and the samples were dried at room temperature for at least 24 h. All specimens were examined with a Zeiss EM 900 transmission electron microscope (Carl Zeiss Microscopy GmbH, Jena, Germany).

2.2.4. Cryo-TEM

Vitrified specimens for cryo-TEM investigations were prepared by a blotting procedure, performed in a chamber with controlled temperature and humidity using an EM GP grid plunger (Leica, Wetzlar, Germany). A drop of the sample solution (c = 3 mM) was placed onto an EM grid coated with a holey carbon film (C-flat, Protochip Inc., Raleight, NC, USA). Excess solution was then removed with a filter paper, leaving a thin film of the solution spanning the holes of the carbon film on the EM grid. Vitrification of the thin film was achieved by rapid plunging of the grid into liquid ethane held just above its freezing point. The vitrified specimens were kept below 108 K during storage, transfer to the microscope, and investigation. Specimens were examined with a Libra 120 Plus TEM (Carl Zeiss Microscopy GmbH, Jena, Germany), operating at 120 kV. The microscope is equipped with a Gatan 626 cryotransfer system and with a BM-2 k-120 Dual-Speed on axis SSCCD-camera (TRS, Moorenweis, Germany).

2.2.5. Freeze-fracture EM (FFEM)

The samples (c = 6 mM) were cryo-fixed using a propane jet-freeze device JFD 030 (BAL-TEC, Balzers, Lichtenstein). Thereafter, the samples were freeze-fractured at −150 °C without etching with a freeze fracture/freeze etching system BAF 060 (BAL-TEC, Balzers, Liechtenstein). The surfaces were shadowed with platinum to produce good topographic contrast (2 nm layer, shadowing angle 45°) and subsequently with carbon to stabilize the ultra-thin metal film (20 nm layer, shadowing angle 90°). The replica were floated in sodium chloride (4%, Roth, Karlsruhe, Germany) for 30 min, rinsed in distilled water (10 min), washed in 30% acetone (Roth, Karlsruhe, Germany) for 30 min, and rinsed again in distilled water (10 min). Thereafter, the replica were mounted on copper grids, coated with formvar film and observed with a transmission electron microscope (LIBRA 120 PLUS, Carl Zeiss Microscopy GmbH, Jena, Germany) operating at 120 kV. Images were taken with a BM-2 k-120 Dual-Speed on axis SSCCD-camera (TRS, Moorenweis, Germany).

2.2.6. Dynamic light scattering (DLS)

DLS experiments were carried out with a Litesizer 500 (Anton Paar GmbH, Graz, Austria). A 3 mW laser with a wavelength of λ = 658 nm and an automatic scattering angle was used. All samples (c = 3 mM) were filled into quartz ultramicro-cuvettes (path length 10 mm). Before starting the measurement, each sample was equilibrated for at least 2 min at 20 °C. Three individual measurements were carried out for each sample with one measurement consisting of 60 runs of 10 s each. Variations of sample viscosities were neglected and the viscosity was assumed to 0.89 mPa s. *Z*-average and polydispersity indices (PdI) were determined by the cumulant analysis software of the instrument. The experimental data were further analysed with the aid of OriginPro 8.

3. Results and discussion

3.1. Mixing studies

To investigate the miscibility of our alkyl-substituted bolalipids **PC-C32(1,32Cn)-PC** (n = 3, 6, 9) with conventional phospholipids, namely DPPC, POPC, and DOPC, the following work scheme was used (Fig. 2).

The bolalipid/phospholipid mixtures were prepared by the film

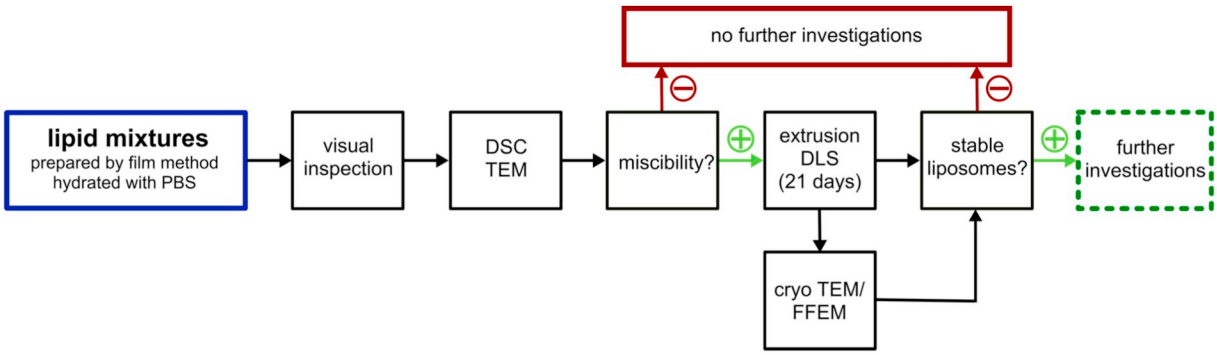

Fig. 2. Schematic representation of work flow for the physicochemical characterization of bolalipid/phospholipid mixtures investigated in this work.

method [38] in the mixing ratios of 1:4, 1:1, and 4:1 (bolalipid:phospholipid, n:n), *i.e.*, 20 mol%, 50 mol%, and 80 mol% of bolalipid, respectively. The lipid films were hydrated with PBS (pH 7.4) to mimic the salt conditions in the human organism. The shape of aggregates was visualized then by TEM and the thermotropic behaviour of the different bolalipid/phospholipid mixtures was characterized by DSC. If a certain miscibility of both lipid components had been observed, the lipid mixtures were extruded through a polycarbonate membrane. To visualize the shape of the liposomes, cryo-TEM and FFEM were used. Finally, the size of produced liposomes was characterized by means of DLS right after the extrusion and after different times of storage. If a bolalipid/phospholipid mixture is identified, which forms storage-stable liposomes, further investigations of these mixed liposomes (bolasomes) will be performed in the near future.

3.1.1. Visual appearance of aqueous bolalipid/phospholipid mixtures

Previous studies regarding the self-assembling properties of the pure single-chain alkyl-branched bolalipids have shown that **PC-C32(1,32C3)-PC** gives a slightly turbid lipid dispersion, which becomes clear upon heating above its phase transition at T_m = 63.2 °C [37]. Due to the formation of sheet-like aggregates of the pure **PC-C32(1,32C3)-PC** at room temperature ($T \approx 22$ °C), we assumed a miscibility with phospholipids. After heating and vortexing, cloudy dispersions were obtained in mixture with DPPC, which became clearer with increasing amount of bolalipid. Furthermore, the appearance of some insoluble particles in the dispersions of all three investigated mixing ratios with DPPC might indicate a segregation of the two lipid components. In mixture with POPC and DOPC, homogenous and opaque dispersions were obtained, which could indicate the formation of vesicular or sheet-like aggregates and hence could predict a miscibility of **PC-C32(1,32C3)-PC** with POPC and DOPC.

PC-C32(1,32C6)-PC shows the formation of fibres both below and above its phase transition temperature at 20.7 °C [37]. Since the well-studied **PC-C32-PC** also aggregates into nanofibres [22,23] and shows no tendency to be incorporated into conventional lipid bilayers [24], we initially did not suspect a pronounced miscibility of **PC-C32(1,32C6)-PC** with phospholipids. All investigated lipid mixtures of **PC-C32(1,32C6)-PC** with phospholipids were homogenous and slightly opaque after heating and vortexing. Again, the mixtures became clearer with increasing amount of bolalipid. The slight turbidity of all dispersions indicated the formation of at least some sheet-like or vesicular aggregates.

PC-C32(1,32C9)-PC self-assembles into fibres below T_m (20.8 °C) and in sheet-like aggregates above T_m [37]. As a result, the dispersion of the pure bolalipid in water becomes turbid upon heating above T_m. All mixtures of **PC-C32(1,32C9)-PC** and phospholipids were homogenous and opaque after heating and vortexing, indicating a certain miscibility of both lipid components.

3.1.2. TEM of negatively stained samples

To visualize the aggregate shapes formed of different bolalipid/phospholipid mixtures in aqueous suspension, EM images of negatively stained samples were prepared. EM images of the 1:4 (*n*:*n*) mixtures, *i.e.*, 20 mol% of bolalipid, are shown in Fig. 3, whereas EM images of the corresponding 4:1 mixtures (80 mol% of bolalipid) are depicted in Fig. S1 (SI, supporting information).

EM images of **PC-C32(1,32C3)-PC** 1:4 mixtures with phospholipids DPPC, POPC, and DOPC revealed the presence of very large sheet-like aggregates of up to several micrometres (Fig. 3A–C). These sheets were sometimes folded or stacked above each other. The shape of aggregates did not change considerably with the use of the different phospholipids. However, closed lipid vesicles (liposomes) were not observed for all three samples. The EM image of **PC-C32(1,32C6)-PC** in mixture with DPPC showed again the formation of sheet-like aggregates (Fig. 3D). By contrast, the mixtures of **PC-C32(1,32C6)-PC** with POPC and DOPC, respectively, revealed the presence of fibrous structures (see black arrow in Fig. 3E) and vesicular assemblies (see black arrowhead in Fig. 3E). In the mixture with DOPC, also larger vesicular structures could be found (see inset in Fig. 3F). Due to the characteristic folding and shape of these lamellar aggregates, we think that these structures were collapsed vesicles rather than flat, sheet-like assemblies [39]. EM images of **PC-C32(1,32C9)-PC** mixtures with DPPC, POPC, and DOPC showed the formation of sheet-like aggregates of different sizes and some vesicular assemblies, independent from the phospholipid used (Fig. 3G–I). However, fibrous aggregates as found for pure **PC-C32(1,32C9)-PC**[37] and **PC-C32(1,32C6)-PC** mixtures with POPC and DOPC, were not observed. This behaviour could be an indication for a miscibility of **PC-C32(1,32C9)-PC** with the different phospholipids used in our mixing experiments.

We then changed the mixing ratio from 1:4 to 4:1, *i.e.* the content of bolalipid was increased from 20 to 80 mol%. With this, we wanted to investigate the influence of the bolalipid content on the shape of aggregates formed in aqueous solution. EM images of the corresponding stained samples are shown in Fig. S1 (SI). By comparing the EM images of both mixing ratios of the appropriate bolalipid/phospholipid mixtures, one could recognize that all the EM images looked virtually the same. Hence, the amount of bolalipid did not have a pronounced impact on the aggregate structure formed in aqueous suspension.

From the results of the EM investigations, we could draw the following conclusions: (i) Whether **PC-C32(1,32C3)-PC** is miscible with various phospholipids or not could not be estimated from the micrographs since both lipid components, *i.e.* the **PC-C32(1,32C3)-PC** and the respective phospholipid, self-assemble into lamellar aggregates by themselves. A phase separation of both lipid component could also be possible within the lamellar structures found for **PC-C32(1,32C3)-PC**/phospholipid mixtures. (ii) **PC-C32(1,32C6)-PC** showed a phase separation in mixtures with POPC and DOPC, respectively, since fibrous and vesicular aggregates were found simultaneously in the EM images of these mixtures. Hence, only a limited miscibility between **PC-C32(1,32C6)-PC** and phospholipids could be deduced so far. (iii) Since **PC-C32(1,32C9)-PC** self-assembles into fibres by themselves and no fibrous aggregates were found in mixture with various phospholipids, a miscibility between both lipid components could be assumed.

3.1.3. DSC measurements

To get information about the thermal behaviour of the different bolalipid/phospholipid mixtures, DSC measurements were conducted. The resulting heating scans of the different mixing ratios (bolalipid:-phospholipid, 1:4, green line; 1:1, orange line; 4:1, blue line) as well as the heating scans of pure lipid components (bolalipid, red line; phospholipid, black line) are shown in Fig. 4. The corresponding transition temperatures could be found in Table S1 (SI).

At first, we discuss the mixtures using the saturated phosphatidylcholine DPPC as phospholipid component. In the case of pure DPPC, the DSC heating scan showed the two well-known endothermic transitions (see black lines in Fig. 4A,D,G): first, the pretransition from the $L_{\beta'}$-phase to the $P_{\beta'}$-phase (ripple-phase) at about 35 °C and, second, the cooperative main transition at 41.9 °C to the liquid-crystalline L_α-phase.

After addition of 20 mol% of **PC-C32(1,32C3)-PC** (Fig. 4A, green line) to DPPC, three transitions at 33.9, 41.6, and 60.6 °C could be detected, which were in the range of T_m of both pure lipid components. With increasing amount of bolalipid, again three transitions could be observed at 41.2, 60.1, and 63.5 °C (Fig. 4A, orange line), while the latter one was exactly located at T_m of pure **PC-C32(1,32C3)-PC**. In the **PC-C32(1,32C3)-PC**:DPPC 4:1 mixture (Fig. 4A, blue line), the temperature values of these transitions slightly changed; only the enthalpy values rose with increasing bolalipid content. The thermal behaviour of the different **PC-C32(1,32C3)-PC**/DPPC mixtures indicated that both lipid components were not miscible, since at least three transitions were observed in the thermograms. It is conceivable that the two lateral *n*-propyl chains of **PC-C32(1,32C3)-PC** were not long enough to fill the void volume, which is created when the bolalipid is inserted in a

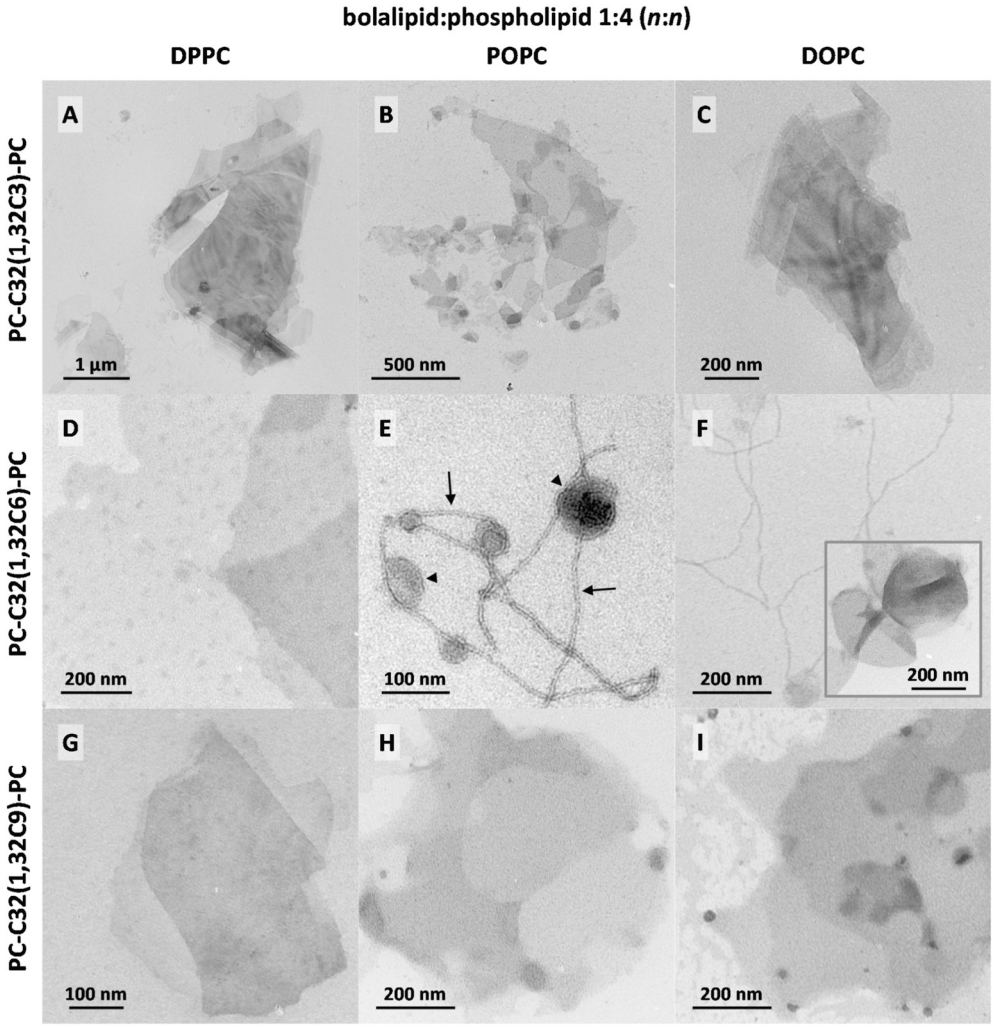

Fig. 3. TEM images of stained aqueous suspensions (c = 120 µM) of bolalipid:phospholipid 1:4 (*n*:*n*) mixtures containing (A–C) **PC-C32(1,32C3)-PC**, (D–F) **PC-C32(1,32C6)-PC**, and (G–I) **PC-C32(1,32C9)-PC** together with (A,D,G) DPPC, (B,E,H) POPC, and (C,F,I) DOPC. In E, the black arrowhead point to vesicular aggregates, whereas the black arrow indicates fibrous structures.

stretched manner into the DPPC bilayer (see Fig. 1) [24]. Hence, both lipid components separated from each other. This 'immiscibility' of both lipids is some kind of remarkable since they self-assemble into lamellar aggregates by themselves; but, a comparable situation is also found for other bolalipid/DPPC mixtures [34].

The **PC-C32(1,32C6)-PC**:DPPC 1:4 and 1:1 mixture again exhibited a complex mixing behaviour since the DSC scan of both lipid mixtures showed three endothermic transitions (Fig. 4D, green and orange line), whereby the high-temperature transition was located slightly below T_m of pure DPPC. The situation changed while using a molar ratio of 4:1. Here, only one transition at 29.4 °C could be detected, 8.6 K above T_m of the pure **PC-C32(1,32C6)-PC** (Fig. 4D, blue line), indicating a certain miscibility between both lipid components at this molar ratio. Using **PC-C32(1,32C9)-PC** in mixture with DPPC, again a non-ideal mixing behaviour could be concluded from the DSC heating scans. In the 1:4 and 1:1 mixture, three or even four transitions could be observed (Fig. 4G, green and orange line), whereas in the 4:1 mixture, only two transitions could be detected (Fig. 4G, blue line). From these investigations we could conclude that the elongation of the lateral alkyl chains of the bolalipid from C3 to C6 and C9, respectively, did not lead to a miscibility with the saturated DPPC. Possibly, only a limited amount of DPPC could be inserted into the bolalipid aggregates, leading either to a thermal stabilization (increased T_m value) in the case of **PC-C32(1,32C6)-PC** or to a slight destabilisation in the case of **PC-C32(1,32C9)-PC**.

In the second mixing experiments, we changed DPPC to POPC bearing one unsaturated alkyl chain. Due to the fluidity of this oleyl chain, a better miscibility with the different bolalipids might be achieved. The DSC heating scan of pure POPC revealed no transition in the temperature range investigated (black lines in Fig. 4B,E,H), due to the simple fact that T_m is around −2 °C [40].

The addition of 20 mol% of **PC-C32(1,32C3)-PC** to POPC led to the occurrence of two small transition peaks in the DSC scan: a very broad one at 54 °C and a second one at 63.5 °C, right at T_m of the pure bolalipid (Fig. 4B, green line). With increasing amount of bolalipid, *i.e.* in the 1:1 and 4:1 mixture, a cooperative transition at 64.5 °C including a low-temperature shoulder at 59.4 °C could be observed (Fig. 5B, orange and blue line). From these thermograms we assume that **PC-C32(1,32C3)-PC** and POPC were not miscible—despite the fact that we did not have any information about possible transition below 5 °C. As a consequence, the unsaturated oleyl chain was not yet sufficient to fill void volume in a postulated 'mixed' **PC-C32(1,32C3)-PC**/POPC bilayer (see Fig. 1).

The situation changes, when **PC-C32(1,32C6)-PC** was mixed with POPC. In the 1:4 mixture, only a very broad transition peak at about 14 °C could be detected (Fig. 4E, green line). Although we could not exclude an additional transition below the measuring range, we assume a miscibility of both lipid components at this molar ratio. In the 1:1

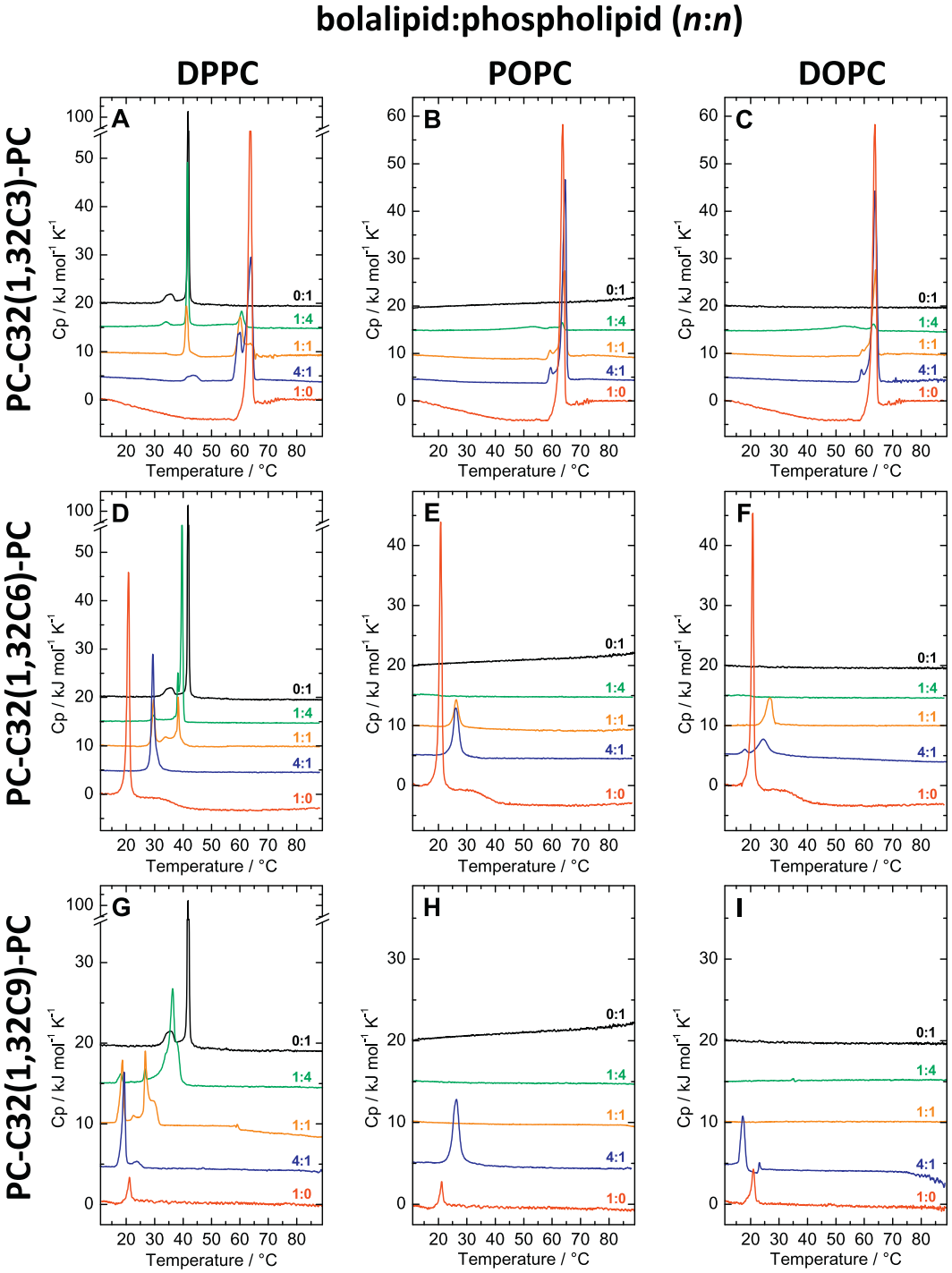

Fig. 4. DSC heating curves of bolalipid/phospholipid mixtures (c = 3 mM in PBS, pH 7.4) containing (A–C) **PC-C32(1,32C3)-PC**, (D–F) **PC-C32(1,32C6)-PC**, and (G–I) **PC-C32(1,32C9)-PC** together with (A,D,G) DPPC, (B,E,H) POPC, and (C,F,I) DOPC, respectively, and a mixing ratio of 1:4 (green lines), 1:1 (orange lines), and 4:1 (blue lines). DSC curves of pure bolalipids (red lines) and phospholipids (black line) are shown for comparison. The curves are shifted vertically for clarity. (For interpretation of the references to colour in this figure legend, the reader is referred to the web version of this article.)

mixture, only one transition at 26.3 °C could be found, 5.5 K above T_m of the pure bolalipid (Fig. 4E, orange line). With a further increasing amount of bolalipid, this transition stayed virtually at the same temperature (Fig. 4E, blue line), only the enthalpy of the transition increased. A comparable situation was found for **PC-C32(1,32C9)-PC**/POPC mixtures. Here, the 1:4 and the 1:1 mixture showed no DSC transition within the temperature range investigated (Fig. 4H, green and orange line), assuming a miscibility between both lipid components at these molar ratios. In the 4:1 mixture, one transition at 26.2 °C could be observed (Fig. 4H, blue line), comparable to T_m of the corresponding **PC-C32(1,32C6)-PC**:POPC mixture. From these results we conclude that (i) **PC-C32(1,32C6)-PC** as well as **PC-C32(1,32C9)-PC** showed a miscibility with POPC and that (ii) an increasing length of the lateral alkyl chain (C6 → C9) led to a higher amount of bolalipid that could be incorporated into a POPC bilayer.

In the third series of mixing experiments, we used DOPC as phospholipid component bearing two unsaturated alkyl chains. With the insertion of a second oleyl chain, an even better miscibility with

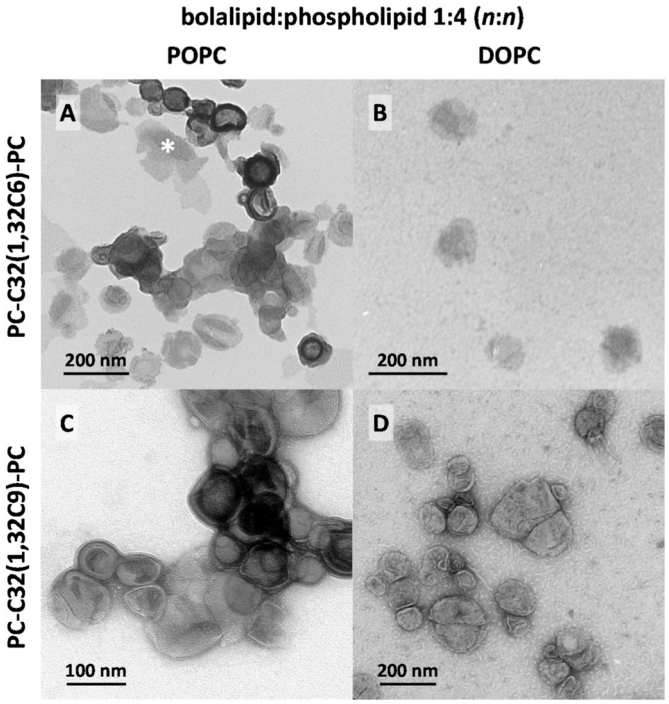

Fig. 5. TEM images of stained aqueous suspensions (c = 120 μM) of extruded bolalipid/phospholipid 1:4 (*n*:*n*) mixtures containing (A,B) **PC-C32(1,32C6)-PC** and (C,D) **PC-C32(1,32C9)-PC** together with (A,C) POPC and (B,D) DOPC. The white asterisk in A points to sheet-like aggregates. Samples were prepared immediately after extrusion.

bolalipids could be expected. Since T_m of DOPC is about −17 °C [41], no transition could be observed in the DSC heating scan (black lines in Fig. 4C,F,I).

The different **PC-C32(1,32C3)-PC**/DOPC mixtures (Fig. 4C) showed virtually the same thermograms compared to the corresponding **PC-C32(1,32C3)-PC**/POPC mixtures (Fig. 4B). The 1:4 mixture revealed a very broad transition peak at about 53 °C and a second one at 63.2 °C (Fig. 4C, green line), whereas the 1:1 and the 4:1 mixture showed a cooperative transition at T_m of pure **PC-C32(1,32C3)-PC** including a small low-temperature shoulder. In accordance to the POPC mixtures, we assume no miscibility between **PC-C32(1,32C3)-PC** and DOPC.

Also the DSC heating scans of **PC-C32(1,32C6)-PC** and **PC-C32(1,32C9)-PC** mixtures with DOPC (Fig. 4F,I) were quite similar to the DSC scans of the corresponding POPC mixtures (Fig. 4E,H), suggesting a comparable mixing behaviour. The **PC-C32(1,32C6)-PC**:DOPC 1:4 mixture revealed a very broad transition at about 17 °C, slightly below T_m of the pure bolalipid (Fig. 4F, green line). In the 1:1 mixture, one transition at 26.8 °C could be found, 6 K above T_m of **PC-C32(1,32C6)-PC** (Fig. 4F, orange line), whereas the 4:1 mixture showed two transitions, a very small one at 18.1 °C and a second one at 24.4 °C (Fig. 4F, blue line). The occurrence of two transitions in the 4:1 mixture was the only difference if the DSC scans of the DOPC and POPC mixtures were compared. An analogous situation was again found for the **PC-C32(1,32C9)-PC**/DOPC mixtures. Here, the 1:4 and the 1:1 mixture revealed no transition within the DSC temperature range (Fig. 4I, green and orange line). Only in the 4:1 mixture, two transitions at 17.3 and 23.1 °C could be detected (Fig. 4I, blue line). Out of these investigations, we draw the same conclusions as postulated for the corresponding POPC mixtures and, in addition, we conclude that the change from POPC to DOPC did not result in a better miscibility with the bolalipids investigated in this work.

Since we observed either a very broad transition peak for the 1:4 mixtures of **PC-C32(1,32C6)-PC** with POPC and DOPC, respectively, or even no transition for the 1:4 and 1:1 mixtures of **PC-C32(1,32C9)-PC** with POPC and DOPC, respectively,—indicating a certain miscibility between both lipid components—we chose these bolalipid/phospholipid mixtures for further investigations regarding the formation of liposomes by extrusion, the morphology of liposomes using different electron microscopic techniques, and the storage stability of these novel bolasomes applying time-dependent DLS measurements.

3.2. Formation and characterization of bolasomes

3.2.1. TEM investigations of stained samples

We used the above mentioned bolalipid/phospholipid mixtures to produce unilamellar liposomes by extrusion through a polycarbonate membrane of 100 nm pore size. Right after extrusion, EM images of negatively stained samples were prepared. The results are shown in Fig. 5, Fig. S2, and Fig. S3 (SI).

EM images of the 1:4 mixtures of **PC-C32(1,32C6)-PC**:POPC/DOPC and **PC-C32(1,32C9)-PC**:POPC/DOPC, respectively, showed the presence of collapsed liposomes in all cases with a diameter between 100 and 200 nm (Fig. 5). Only the **PC-C32(1,32C6)-PC**:POPC mixture revealed the formation of some sheet-like structures (see white asterisk in Fig. 5A). EM images of the **PC-C32(1,32C9)-PC**:POPC/DOPC 1:1 mixtures also showed the formation of vesicular structures (Fig. S2, SI); however, in the **PC-C32(1,32C9)-PC**:DOPC 1:1 mixture, also some traces of fibrous aggregates could be detected (Fig. S3, SI). The latter finding is kind of remarkable, since we did not observe any transition peak in the corresponding DSC measurement (see Fig. 4I, orange line) and we therefore assume a miscibility of both lipid components at this mixing ratio.

Since we observed vesicular and fibrous aggregates for the **PC-C32(1,32C6)-PC**:POPC/DOPC 1:4 mixtures prior and only vesicular structures after the extrusion (compare Fig. 3E,F with Fig. 5A,B), the question arose, if the fibrous aggregates could be withheld by the polycarbonate membrane during extrusion. To clarify this fact, we additionally performed DSC measurements of **PC-C32(1,32C6)-PC**/POPC mixtures with different bolalipid content right after the extrusion and compare the enthalpy values obtained with the values from the DSC scans prior extrusion (data not shown). We came to the conclusion that there was indeed a loss of bolalipid when the bolalipid/phospholipid mixtures were extruded. However, the loss decreased with decreasing amount of bolalipid in the mixture, *i.e.* the loss of bolalipid in the 1:1 mixture was much lower compared to the loss of bolalipid in the corresponding 4:1 mixture. Due to the simple fact that we did not observe a DSC transition of the corresponding **PC-C32(1,32C6)-PC**:POPC 1:4 mixture, we could not measure the loss of bolalipid using this mixing ration. But, we presume that the loss of bolalipid in the 1:4 mixture (including 20 mol% of bolalipid) could be neglected and that almost everything of the bolalipid added was incorporated in the extruded bolalipid/POPC bilayer.

Since some of the 1:1 mixtures showed the formation of fibrous aggregates (see Fig. S3, SI), we concentrate our further studies on the 1:4 mixtures of **PC-C32(1,32C6)-PC**:POPC/DOPC and **PC-C32(1,32C9)-PC**:POPC/DOPC, respectively.

3.2.2. Cryo-TEM and FFEM investigations

To further study the shape of liposomes formed of the 1:4 bolalipid/phospholipid mixtures mentioned above, we recorded micrographs of vitrified specimens and of replica of freeze-fractured samples. The application of vitrified samples for cryo-EM has advantages compared to TEM of stained samples [39]. Whereas the drying procedure during preparation of stained samples could lead to artefacts, cryo-TEM of vitrified specimens preserves the shape of the aggregates. Moreover, with the use of FFEM, one can investigate the morphology of fractured vesicles in more detail. We therefore prepared cryo-TEM samples of the four bolalipid/phospholipid 1:4 mixtures in PBS at pH 7.4 and, in addition, FFEM samples of the two corresponding DOPC mixtures. The results are shown in Fig. 6 and Fig. 7.

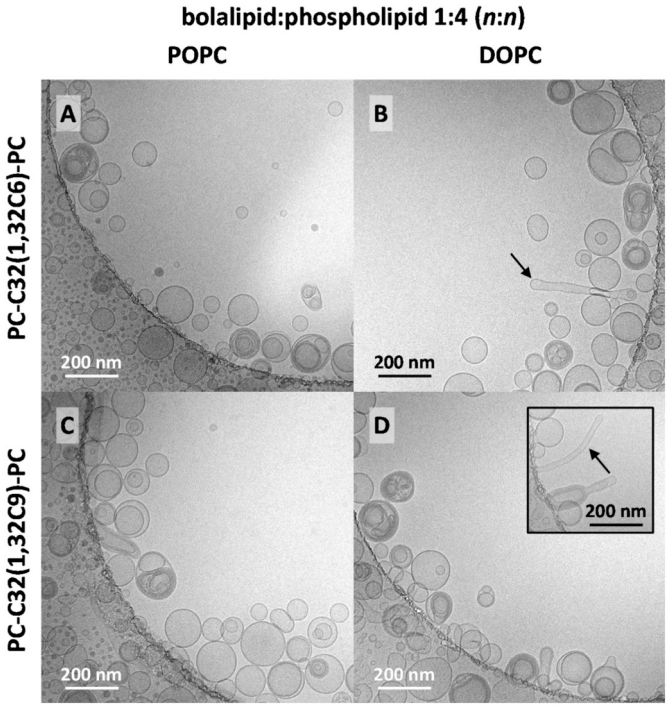

Fig. 6. Cryo-electron micrographs of an aqueous suspension (c = 3 mM, PBS at pH 7.4) of bolalipid/phospholipid 1:4 mixtures containing (A,B) **PC-C32(1,32C6)-PC** and (C,D) **PC-C32(1,32C9)-PC** together with (A,C) POPC and (B,D) DOPC. The black arrows in B and D (inset) point to elongated liposomes. Lipid samples were extruded through a 100 nm membrane.

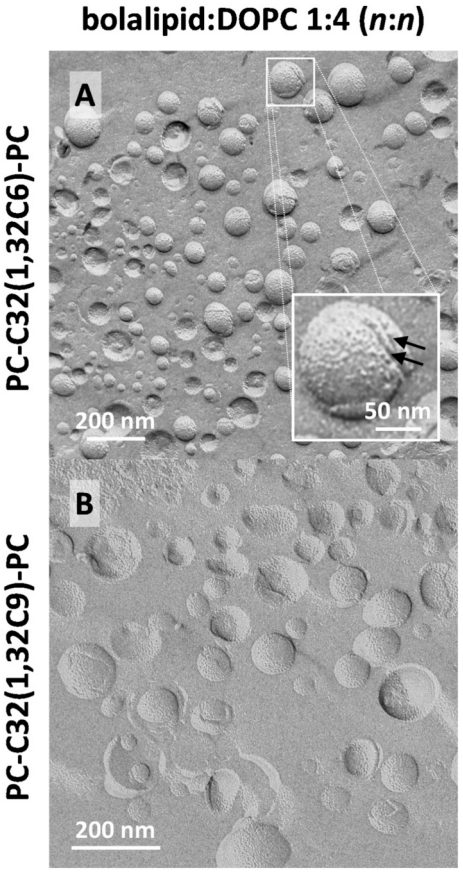

Fig. 7. Electron microscopic images of replica of freeze-fractured samples of liposomes composed of aqueous suspensions (c = 6 mM, PBS at pH 7.4) of (A) **PC-C32(1,32C6)-PC**:DOPC (1:4, *n*:*n*), (B) **PC-C32(1,32C9)-PC**:DOPC (1:4, *n*:*n*). The inset in A shows a magnification of a liposome with cross-fracturing.

Cryo-TEM images of all extruded **PC-C32(1,32C6)-PC** and **PC-C32(1,32C9)-PC** 1:4 mixtures using POPC and DOPC, respectively, revealed the presence of many unilamellar vesicles with diameters of up to 200 nm (Fig. 6A–D). In addition, some oligolamellar and multilamellar vesicles as well as few multivesicular vesicles could be found. The fact that no fibrous aggregates were found in all of the four samples confirmed our assumption that the bolalipid and the phospholipid were miscible at that molar ratio, leading to mixed liposomes (bolasomes). Interestingly, in both mixtures using DOPC, a small number of elongated liposomes could be observed (black arrows in Fig. 6B,D). A comparable behaviour is already found for other bolalipid/DOPC mixtures using artificial glycerol diether bolalipids [42]. Such elongated vesicular structures are also described for different phospholipid/cholesterol mixtures [43,44]. The reasons therefor could be found in the presence of packing defects or in a partial segregation of both lipid components within one aggregate. The latter is already confirmed by Xu and co-workers, who showed that in liposomes composed of phosphatidylcholines and ceramides, both lipid components tend to separate within one lipid aggregate due to different transition temperatures [45]. Hence, a partial stiffness of the liposomal bilayer, due to a higher T_m of ceramides, triggers the formation of such elongated liposomes—an explanation, which could also be applied to our bolalipid/DOPC mixtures.

From the extruded **PC-C32(1,32C6)-PC**:DOPC and **PC-C32(1,32C9)-PC**:DOPC 1:4 mixtures, respectively, we also prepared replica of freeze-fractured samples for EM investigations. The resulting micrographs are shown in Fig. 7.

Both samples contained vesicles with a diameter of up to 200 nm. Major differences in liposome morphology in both samples could not be detected. The fracture surface showed no distinct difference between the inner and outer side of the mixed liposomes. Fracturing occurred along the surface of the vesicles as no inner fracture faces could be observed. Such inner fracture faces would appear when bilayer membranes of conventional phospholipids are fractured [46]. The absence of inner fracture faces is evidence for a membrane-spanning fashion of the bolalipid within the DOPC bilayer and for the assumption that both lipid components, bolalipid and phospholipid, are miscible at the 1:4 mixing ratio. The alternative U-shaped conformation of the bolalipid leads to higher energy due to bending of the alkyl chain and is therefore unlikely. In a bilayer arrangement this would lead to the occurrence of inner fracture faces, which were not seen.

In the case of oligolamellar liposomes (see inset in Fig. 7A), the fracture runs along the outer surface of the outer membrane before cross-fracturing occurred and the fracture continued along the outer membrane of the inner vesicle. Here, the thickness of the mixed lipid bilayer could be determined to be 4–6 nm, which roughly corresponds to the length of one bolalipid molecule and to the thickness of a DOPC bilayer [47,48].

Another noticeable fact was the occurrence of a rough surface of the mixed liposomes in comparison to the smooth surface of the surrounding ice. This phenomenon was found for both bolasomes in two independent preparations (Fig. 7A,B). In earlier studies, Beveridge et al. made a similar observation in archaeosomes with an increasing amount of membrane-spanning tetraether lipids: [49] while archaeosomes composed of diether lipids, which are arranged in a bilayer, show smooth surfaces, a rough surface is observed using archaeosomes with tetraether lipids. They claimed that these rough structures are due to the occurrence of tetraether lipid complexes. Hence, the rough surface of our bolasomes is a further evidence for the incorporation of the artificial single-chain alkyl-branched bolalipids into DOPC liposomes.

From the results of the EM investigations shown above, we could now conclude that **PC-C32(1,32C6)-PC** and **PC-C32(1,32C9)-PC** can be incorporate to 20 mol% into POPC and DOPC bilayers by

maintaining their liposomal structure.

3.2.3. DLS measurements

To finally check the storage stability of our new bolasomes, we measured their particle size (z-average) and their particle size distribution (polydispersity index, PdI) immediately after extrusion (day 0) and after different times of storage at 4 °C (day 1, day 7, and day 21).

The DLS data for a **PC-C32(1,32C6)-PC**:DOPC 1:4 mixture at day 0 are exemplarily shown in Fig. S4 (SI). The autocorrelation function (Fig. S4A, scattered data) was analysed using the cumulant fit (Fig. S4A, red line), from which we could get the hydrodynamic diameter (z-average) for the liposomal aggregates and the PdI. For the **PC-C32(1,32C6)-PC**:DOPC 1:4 mixture, a z-average of 134 nm and a PdI of 0.09 were obtained, whereby PdI-values below 0.1 can be assumed as monodisperse [50]. In the case the PdI is above 0.1, the analysis of DSL data by a cumulant fit can become unreliable and an alternative algorithm, such as an exponential regularised fit together with non-negative least squares (NNLS), is applied instead [50]. Using this method, a distribution of different particle size populations is obtained. As an example, the mass-weighted particle size distribution of the **PC-C32(1,32C6)-PC**:DOPC 1:4 mixture at day 0 is shown in Fig. S4B indicating a monodisperse particle size distribution between 70 and 240 nm with a maximum at around 100 nm. These results were in line with our EM investigations.

The results of the long-term storage assay of the four novel bolalipid/phospholipid liposomes using DLS are summarized in Fig. 8. First, and this is quite remarkable, the z-average values of all mixed liposomes were in the range of 120–140 nm over the whole period of storage time (21 days; see bars in Fig. 8). We did not observed any trend of increasing or decreasing size upon storage, which could be due to separation or agglomeration processes. For both **PC-C32(1,32C9)-PC** mixtures, also the PdI values did not change during storage. Only for the corresponding **PC-C32(1,32C6)-PC** mixtures, the PdI values slightly increased over time to 0.10–0.16, but, the analysis using NNLS could always confirm a monodisperse particle size distribution (data not shown). Thus, these results confirmed the storage stability of our novel mixed liposomes for at least three weeks.

4. Conclusions and summary

The development of stabilized vesicles (liposomes), which can protect their cargo from the harsh conditions found in the gastrointestinal tract, is of great importance for oral drug delivery purposes. The use of bipolar lipids (bolalipids), which can span and hence stabilize a phospholipid bilayer, is a promising approach to enhance the integrity of lipid vesicles. However, earlier studies have shown that unmodified single-chain bolalipids, such as **PC-C32-PC**, cannot be used as stabilizer of phospholipid bilayers [24]. If **PC-C32-PC** is incorporated in a stretched manner into, *e.g.* a DPPC or POPC bilayer, void volume is created, which is energetically unfavourable and lead, in consequence, to a separation into bolalipid fibres and phospholipid liposomes (see Fig. 1).

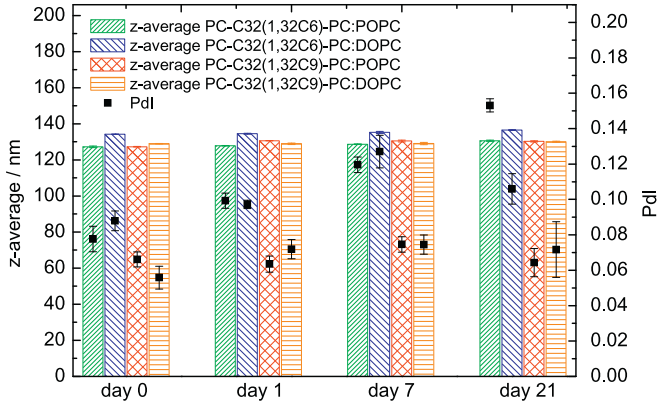

Fig. 8. Data of DLS measurements: influence of the time of storage (at 4 °C) on the particle size: mean and s.d. (n = 3) of z-average (bars) and polydispersity index PdI (black squares) of a **PC-C32(1,32C6)-PC**:POPC 1:4 mixture (green bars), a **PC-C32(1,32C6)-PC**:DOPC 1:4 mixture (blue bars), a **PC-C32(1,32C9)-PC**:POPC 1:4 mixture (red bars), and a **PC-C32(1,32C9)-PC**:DOPC 1:4 mixture (orange bars), respectively, are shown. The concentration of all lipid mixtures was 3 mM in PBS pH 7.4. (For interpretation of the references to colour in this figure legend, the reader is referred to the web version of this article.)

To circumvent these packing frustrations, a set of novel single-chain alkyl-branched bolalipids (**PC-C32(1,32C*n*)-PC**) have been synthesized bearing lateral alkyl chains of different length (n = 3, 6, or 9) right next to the two PC headgroups [37]. The insertion of longer alkyl side chains was not possible so far due to synthetical limitations. With the introduction of side chains, we wanted to answer the following questions: (i) Are these side chains sufficient to fill the void volume and to generate a miscibility between these bolalipids and bilayer-forming phospholipids by maintaining the liposomal structure of the mixed lipid systems? (ii) Is there a relationship between the length of the lateral alkyl chains of the bolalipid and the degree of miscibility? To answer these questions, a set of different mixing experiments of our new bolalipids with either saturated (DPPC) or unsaturated (POPC, DOPC) phospholipids were conducted, which are presented in this study.

PC-C32(1,32C3)-PC bearing the shortest lateral chains showed no or a very limited miscibility with all three phospholipids. It is conceivable that the C3 side chain was not long enough to fill the void volume. As a consequence—even though only large sheet-like structures, *i.e.* one type of aggregate, were found in EM images—bolalipid and phospholipid were separated from each other.

The same situation was found for **PC-C32(1,32C6)-PC** and **PC-C32(1,32C9)-PC** in mixtures with DPPC. In the case of an excess of phospholipid, a complex thermal behaviour was observed in the DSC heating scans showing up to four transitions. This phenomenon could be explained as a separation of both lipid components into a 'bolalipid-rich' phase, a 'phospholipid-rich' phase, and possibly a third 'mixed' phase. However, since only sheet-like aggregates could be found in the corresponding EM images, a separation of both lipid components within the same aggregate is conceivable. A comparable situation is found for another bolalipid/DPPC mixtures described previously [51]. But the absence of fibrous aggregates in the EM images of the bolalipid/DPPC mixtures—and **PC-C32(1,32C6)-PC** as well as **PC-C32(1,32C9)-PC** self-assemble into fibres by themselves[37]—led to a second conclusion: A small amount of DPPC could be incorporated into the bolalipid aggregate leading to the formation of sheet-like structures, *i.e.* to the occurrence of a fibre-to-sheet transformation by the addition of small amounts of DPPC. This result is in contrast to earlier studies using **PC-C32-PC**/DPPC mixtures, where the nanofibres of **PC-C32-PC** are stabilized by the insertion of DPPC molecules [24]. This finding is also supported by the fact that the corresponding DSC heating scan of the lipid mixtures including an excess of bolalipid showed only one or two transitions. Hence, a limited amount of DPPC could be incorporated into aggregates of **PC-C32(1,32C6)-PC** and **PC-C32(1,32C9)-PC**.

The situation changed if bolalipids bearing longer lateral alkyl chains, **PC-C32(1,32C6)-PC** and **PC-C32(1,32C9)-PC**, were mixed with unsaturated phospholipids. Both bolalipids showed a miscibility with POPC and DOPC, respectively, and the amount of bolalipid that could be incorporated into a phospholipid bilayer increased with increasing length of the lateral alkyl chains of the bolalipid. Hence, a certain length of the bolalipid' side chains and the use of unsaturated phospholipids were necessary to induce a miscibility between both lipid components. Both structural elements seemed to be able to fill the void volume in a mixed lipid bilayer (see Fig. 1) leading to energetically favourable conditions for a mixing of bolalipids with phospholipids.

Finally, we used **PC-C32(1,32C6)-PC**:POPC/DOPC and **PC-C32(1,32C9)-PC**:POPC/DOPC mixtures including 20 mol% of the

corresponding bolalipid to produce liposomes (bolasomes) by extrusion. Within these novel bolasomes, the bolalipids might cluster since a rough surface of the liposomes was shown in electron micrographs of replica of freeze-fractured samples. But, these vesicles were stable in size upon storage at 4 °C for at least three weeks, and liposomes including **PC-C32(1,32C9)-PC** were also stable in their size distribution. Hence, the bolalipid bearing the longest (C9) lateral alkyl chain is recommended for further studies regarding the production of bolasomes.

To summarize, we were able to show that single-chain alkyl-branched bolalipids were miscible with unsaturated bilayer-forming phospholipids; a fact, which was shown—to our knowledge—for the first time for artificial single-chain bolalipids. Moreover, the degree of miscibility could be tuned by the length of the lateral alkyl chain of the bolalipid. The results described in this work are the basis for further studies: Investigations, such as permeability assays, *in vitro* digestion assays, and dye release experiments, regarding the stability of our novel bolasomes under conditions found in the gastrointestinal tract are currently under way. If these pursuing studies will show an increased stability/integrity of our bolasomes, an application as oral drug delivery vehicles is envisaged.

Notes

The authors declare no competing financial interest.

Acknowledgment

This work was financially supported by grants from the Phospholipid Research Center Heidelberg (to S.M.), by grants from the Deutsche Forschungsgemeinschaft (DFG) project DR 1024/1-1 (to K.G. and S.D.), and by grants from the Freundeskreis für Pharmazie e.V. (to M.K.). The authors thank Annekatrin Rother (Institute of Biochemistry, Martin Luther University Halle-Wittenberg, Germany) for her support in collecting the multitude of EM images and Simone Fraas (Biocenter, Martin Luther University Halle-Wittenberg, Germany) for making the freeze fracture replica.

Appendix A. Supplementary data

Additional EM investigations, DSC data, and DLS measurements. Supplementary data to this article can be found online at https://doi.org/10.1016/j.bpc.2018.10.003.

References

[1] J.-H. Fuhrhop, T. Wang, Chem. Rev. 104 (2004) 2901–2937.
[2] M. De Rosa, A. Gambacorta, A. Gliozzi, Microbiol. Rev. 50 (1986) 70–80.
[3] K. Yamauchi, K. Doi, M. Kinoshita, F. Kii, H. Fukuda, Biochim. Biophys. Acta Biomembr. 1110 (1992) 171–177.
[4] C.G. Choquet, G.B. Patel, T.J. Beveridge, G.D. Sprott, Appl. Microbiol. Biotechnol. 42 (1994) 375–384.
[5] C.G. Choquet, G.B. Patel, G.D. Sprott, Can. J. Microbiol. 42 (1996) 183–186.
[6] D.A. Brown, B. Venegas, P.H. Cooke, V. English, P.L.-G. Chong, Chem. Phys. Lipids 159 (2009) 95–103.
[7] S.M. Jensen, C.J. Christensen, J.M. Petersen, A.H. Treusch, M. Brandl, Int. J. Pharm. (Amsterdam, Neth.) 493 (2015) 63–69.
[8] J. Parmentier, B. Thewes, F. Gropp, G. Fricker, Int. J. Pharm. 415 (2011) 150–157.
[9] G. Mahmoud, J. Jedelska, B. Strehlow, U. Bakowsky, Eur. J. Pharm. Biopharm. 95 (2015) 88–98.
[10] P. Uhl, F. Helm, G. Hofhaus, S. Brings, C. Kaufman, K. Leotta, S. Urban, U. Haberkorn, W. Mier, G. Fricker, Eur. J. Pharm. Biopharm. 103 (2016) 159–166.
[11] P. Uhl, S. Pantze, P. Storck, J. Parmentier, D. Witzigmann, G. Hofhaus, J. Huwyler, W. Mier, G. Fricker, Eur. J. Pharm. Sci. 108 (2017) 111–118.
[12] G.B. Patel, G.D. Sprott, Crit. Rev. Biotechnol. 19 (1999) 317–357.
[13] T. Eguchi, H. Kano, K. Arakawa, K. Kakinuma, Bull. Chem. Soc. Jpn. 70 (1997) 2545–2554.
[14] T. Eguchi, K. Arakawa, T. Terachi, K. Kakinuma, J. Org. Chem. 63 (1998) 8080.
[15] T. Eguchi, K. Ibaragi, K. Kakinuma, J. Org. Chem. 63 (1998) 2689–2698.
[16] S. Drescher, A. Meister, A. Blume, G. Karlsson, M. Almgren, B. Dobner, Chem. Eur. J. 13 (2007) 5300–5307.
[17] S. Drescher, A. Meister, G. Graf, G. Hause, A. Blume, B. Dobner, Chem. Eur. J. 14 (2008) 6796–6804.
[18] A. Jacquemet, J. Barbeau, L. Lemiègre, T. Benvegnu, Biochimie 91 (2009) 711–717.
[19] T. Markowski, S. Drescher, G. Foerster, B.-D. Lechner, A. Meister, A. Blume, B. Dobner, Langmuir 31 (2015) 10683–10692.
[20] G. Leriche, J.L. Cifelli, K.C. Sibucao, J.P. Patterson, T. Koyanagi, N.C. Gianneschi, J. Yang, Org. Biomol. Chem. 15 (2017) 2157–2162.
[21] Z. Huang, D.M. Zhao, X. Deng, J. Zhang, Y.M. Zhang, X.Q. Yu, Nanomaterials (Basel) 8 (2018).
[22] K. Köhler, G. Förster, A. Hauser, B. Dobner, U.F. Heiser, F. Ziethe, W. Richter, F. Steiniger, M. Drechsler, H. Stettin, A. Blume, Angew. Chem. Int. Ed. 43 (2004) 245–247.
[23] K. Köhler, G. Förster, A. Hauser, B. Dobner, U.F. Heiser, F. Ziethe, W. Richter, F. Steiniger, M. Drechsler, H. Stettin, A. Blume, J. Am. Chem. Soc. 126 (2004) 16804–16813.
[24] A. Meister, K. Koehler, S. Drescher, B. Dobner, G. Karlsson, K. Edwards, G. Hause, A. Blume, Soft Matter 3 (2007) 1025–1031.
[25] A. Blume, S. Drescher, G. Graf, K. Koehler, A. Meister, Adv. Colloid Interf. Sci. 208 (2014) 264–278.
[26] T. Markowski, S. Drescher, A. Meister, G. Hause, A. Blume, B. Dobner, Eur. J. Org. Chem. (2011) 5894–5904.
[27] T. Markowski, S. Drescher, A. Meister, A. Blume, B. Dobner, Org. Biomol. Chem. 12 (2014) 3649–3662.
[28] M. Berchel, T. Le Gall, O. Lozach, J.P. Haelters, T. Montier, P.A. Jaffres, Org Biomol Chem 14 (2016) 2846–2853.
[29] G. Graf, S. Drescher, A. Meister, V.M. Haramus, B. Dobner, A. Blume, J. Colloid Interface Sci. 393 (2013) 143–150.
[30] A. Blume, S. Drescher, A. Meister, G. Graf, B. Dobner, Faraday Discuss. 161 (2013) 193–213.
[31] S. Drescher, K. Helmis, A. Langner, B. Dobner, Monatsh. Chem. 141 (2010) 339–349.
[32] S. Drescher, S. Becker, B. Dobner, A. Blume, RSC Adv. 2 (2012) 4052–4054.
[33] S. Drescher, S. Sonnenberger, A. Meister, A. Blume, B. Dobner, Monatsh. Chem. 143 (2012) 1533–1543.
[34] S. Drescher, B.-D. Lechner, V.M. Garamus, L. Almasy, A. Meister, A. Blume, Langmuir 30 (2014) 9273–9284.
[35] S. Drescher, A. Meister, V.M. Garamus, G. Hause, C.J. Garvey, B. Dobner, A. Blume, Eur. J. Lipid Sci. Technol. 116 (2014) 1205–1216.
[36] S. Drescher, V.M. Garamus, C.J. Garvey, A. Meister, A. Blume, Beilstein J. Org. Chem. 13 (2017) 995–1007.
[37] K. Gruhle, S. Mueller, A. Meister, S. Drescher, Org. Biomol. Chem. 16 (2018) 2711–2724.
[38] A.D. Bangham, M.M. Standish, J.C. Watkins, J. Mol. Biol. 13 (1965) 238–252.
[39] A. Meister, A. Blume, Polymers 9 (2017) 521.
[40] H. Pfeiffer, G. Klose, K. Heremans, Chem. Phys. Lett. 572 (2013) 120–124.
[41] Z.V. Leonenko, E. Finot, H. Ma, T.E.S. Dahms, D.T. Cramb, Biophys. J. 86 (2004) 3783–3793.
[42] S. Mueller, A. Meister, C. Otto, G. Hause, S. Drescher, Biophys. Chem. 238 (2018) 39–48.
[43] D. Momekova, G. Momekov, S. Rangelov, G. Storm, N. Lambov, Soft Matter 6 (2010) 591–601.
[44] M. Almgren, K. Edwards, G. Karlsson, Colloids Surf. A Physicochem. Eng. Asp. 174 (2000) 3–21.
[45] P. Xu, G. Tan, J. Zhou, J. He, L.B. Lawson, G.L. McPherson, V.T. John, Langmuir 25 (2009) 10422–10425.
[46] L.D. Mayer, M.J. Hope, P.R. Cullis, Biochim. Biophys. Acta 858 (1986) 161–168.
[47] J. Gallova, D. Uhrikova, A. Islamov, A. Kuklin, P. Balgavy, General Physiology and Biophysics, Vol. 23 (2004), pp. 113–128.
[48] N. Kučerka, M.-P. Nieh, J. Katsaras, Biochim. Biophys. Acta Biomembr. 2011 (1808) 2761–2771.
[49] T.J. Beveridge, C.G. Choquet, G.B. Patel, G.D. Sprott, J. Bacteriol. 175 (1993) 1191–1197.
[50] P.A. Hassan, S. Rana, G. Verma, Langmuir 31 (2015) 3–12.
[51] T. Markowski, S. Müller, B. Dobner, A. Meister, A. Blume, S. Drescher, Polymers 9 (2017) 573.